Atmospheric Radiation Monitor

M.A. Leigui de Oliveira*, C.J. Todero Peixoto*, M.S.A.B. Leão*, R.M. Lima*, E.F. Lima*, V.P. Luzio*, N.T.S. Ribeiro*, A.F. Barbosa†, H.P. Lima Jr†, L.M. de Andrade Filho†, A.B. Vilar†, E. Kemp‡ and L.F.G. Gonzales‡

*Centro de Ciências Naturais e Humanas, Universidade Federal do ABC (UFABC), Santo André, SP, Brazil
†Laboratório de Sistemas de Detecção, Centro Brasileiro de Pesquisas Físicas (CBPF), Rio de Janeiro, RJ, Brazil
‡Instituto de Física Gleb Wataghin, Universidade Estadual de Campinas (UNICAMP), Campinas, SP, Brazil

Abstract. **The Atmospheric Radiation Monitor (MonRAt) is a compact experiment aiming to measure the fluorescence radiation in the atmosphere initiated by cosmic rays with energies between 100 PeV and 100 EeV. It is composite by a mirror focusing on a multianodic photomultiplier with an ultraviolet filter - selecting photons with wavelengths between 300 and 450 nm - and the data acquisition boards. The monitor is intended to contribute in problems such as the study of fluorescence radiation yield in the atmosphere parameterized with atmospheric conditions.**

Keywords**: Cosmic rays. Extensive air showers. Atmospheric fluorescence.**

I. INTRODUCTION

Primary cosmic ray (CR) particles colide with atomic nuclei in high altitudes of the atmosphere generating, through nuclear and electromagnetic processes, secondary particles which can travel and colide with other nuclei. The number of particles increases and reaches a maximum. Then, decreases when the particles start to lose their energy though ionization and excitation of air atoms and molecules. This cascade, formed by the passage of a cosmic ray through the atmosphere, is called Extensive Air Shower (EAS). In the shower path down to Earth's surface, the nitrogen molecules are excited, mainly by the charged particles of the EAS electromagnetic component, i.e., electrons and positrons. Fluorescence light is generated by the deexcitation of nitrogen molecules and this radiation is isotropically emitted with a wavelength spectrum between 300 and $450\ nm$ (see Fig.1). The detection of EAS using nitrogen fluorescence light has been demonstrated to be successful in the end of 60's [1] and nowadays is a well established technique, important for several experiments in course [2], [3], [4] or in planning [5], [6], [7]. The atmosphere is used as a giant scintillator which gives informations about the the EAS longitudinal development. This development, in turn, can be used to estimate the energy and the composition of the primary CRs. The ammount of fluorescence light created by a huge number of electrons is intense enough to be detected even by photomultipliers placed some kilometers away from the emission point. As an example, a primary of $10\ EeV$ will produce a cascade with 6 billions electrons near the EAS maximum and will dissipate approximately $0.1\ J$ in $30\ \mu s$.

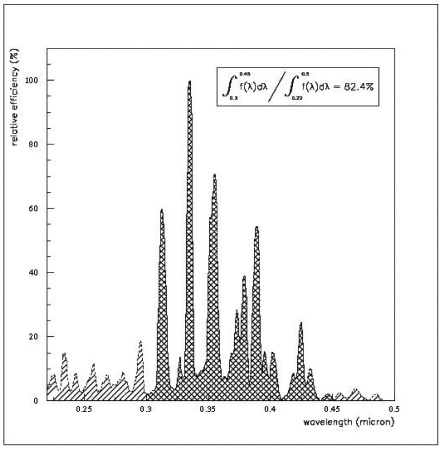

Fig. 1. Spectrum of N_2 fluorescence emissions (bands: 2P molecular and 1N of ion N_2^+).

To perform the EAS measurements, the fluorescence yield must be parameterized with air composition and physical properties like density, pressure and temperature, from the ground level up to high altitudes. Absolute fluorescence yield is known with uncertainty around 1% for some electron energies and some air pressures and temperatures [8], [9], [10], [11], [12], [13]. The extrapolation of these results are in present the main source of systematic errors in the determination of EAS parameters by fluorescence telescopes [14]. The fluorescence yield is proportional to charged particles energy deposit in air and varies from 3.0 to $5.6\ fotons/m$ per charged particle as a function of altitude. Thus, for a given shower development depth (altitude h within Δx), one can calculate the number of fluorescence photons at the shower axis by:

$$N_\gamma(h) = Y(\lambda, p, T) \cdot \Delta x \qquad (1)$$

where $Y(\lambda, p, T)$ is fluorescence yield which depends on the wavelength (Fig.1), pressure and temperature and Δx is the transversed path.

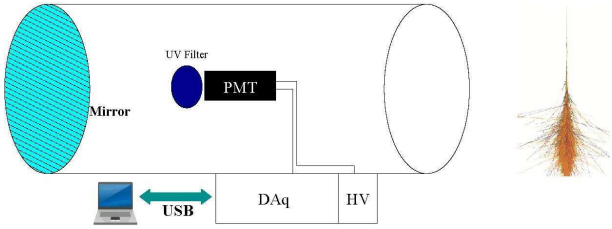

Fig. 2. Schematic diagram of MonRAt.

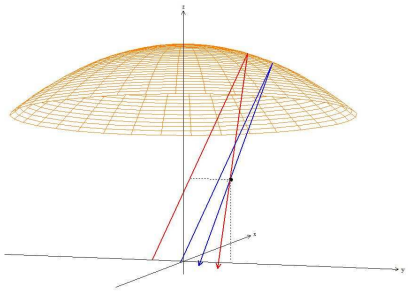

Fig. 3. Ray-tracing software simulating photons reflecting on a parabolic mirror and arriving at the photocathode position.

II. The MonRAt concept

The Atmospheric Radiation Monitor [15] (MonRAt[1]) is a compact telescope aiming to measure fluorescence radiation generated by showers in the energy region $10^{17}\ eV < E < 10^{20}\ eV$. The detector components can be easily replaced and their performances studied in details.

The detection principle of MonRAt is illustrated in Fig.2. It consists of a multianodic photomultiplier (PMT) — Hamamatsu M64 of 8×8 pixels — at the focus of a parabolic mirror mounted in a newtonian telescope setup. In front of the PMT field of view filters will be positioned to select light with wavelength in the near ultraviolet region: a broad band filter or selecting one of the main peaks of N_2 emissions. The mirror geometry limits the optical aberrations and the spot at the focus cannot be bigger in area than one PMT pixel ($2\times2mm^2$). A detailed ray-tracing has been performed to select the geometrical parameters of the telescope (see Fig.3 and Fig.4).

The Data Acquisition (DAq) system will consist of 4 FPGA-based boards (called MPDs) able to record trigger times and wave forms from each pixel. We measure the delay between the triggered signals from the anodes and a time reference which is set to be the instant of the PMT's 12^{th} dynode trigger. These time intervals are measured through TDCs with $5\ ns$ of resolution. The analogic measurements in turn are done with resolution of 12 bits and sample rate of $60\ MSPS$. The data are sent to a computer by a USB port. A prototype of the DAq board is shown in Fig.5.

Preliminary tests have been performed in order to design the front-end electronics and we tested different

[1]From the Portuguese, Monitor de Radiação Atmosférica.

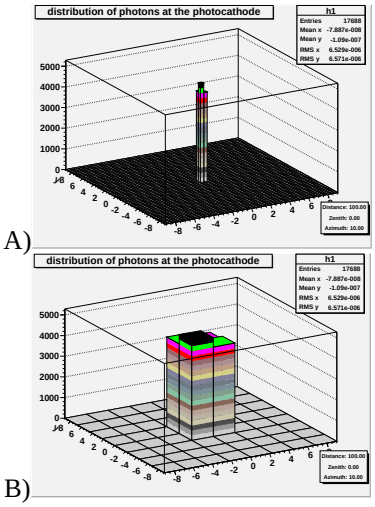

Fig. 4. Distributions of photons arrival positions at the photocathode for: A) an arbitrary resolution; B) a 8×8 pixels matrix.

Fig. 5. Photograph of a MPD prototype.

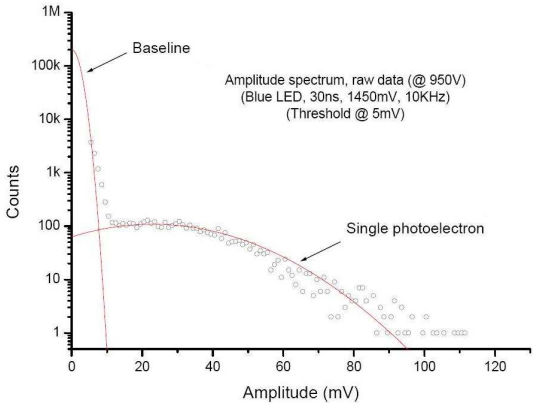

Fig. 6. Single photon spectrum.

pre-amplifiers circuits. The MPDs saturates at $1\ V$, therefore is preferable to observe single photon peak at low amplitudes ($\sim 30\ mV$) such that the dynamical range of MPD can cover as many photons as possible. In Fig.6, we present the single photon spectrum for a blue led flashing at the central pixel with a frequency of $10\ kHz$. The PMT high voltage was set to $950\ V$ and we estimate a gain of 1.5×10^6, in accordance to the manufactor specifications [16].

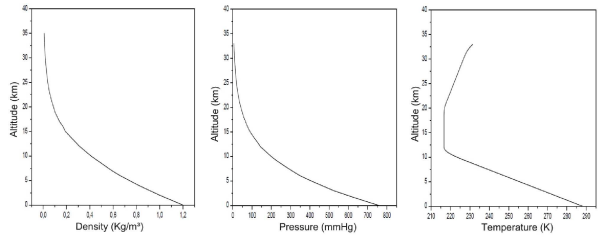

Fig. 7. Parameterization of the atmosphere used in simulations [19].

III. SIMULATIONS

A library of showers simulated by CORSIKA [17] — using version 6.5021 and hadronic model SIBYLL 2.1 [18] — has been produced. For seven fixed energies (10^{17}, $10^{17.5}$, 10^{18}, $10^{18.5}$, 10^{19}, $10^{19.5}$ and $10^{20}\ eV$), we simulated 1000 showers initiated by protons. The particles are observed from the top of the atmosphere until the sea level with longitudinal development in steps of $5\ g/cm^2$. The zenith angles were sorted between 0 and $60°$ and we applied a thinning factor of 10^{-5}.

The number and the distribution energy of electrons and positrons have been read for each shower at several longitudinal levels, defined in steps of $5\,g/cm^2$. Taking into account a detailed parameterization of the atmosphere up to $35\,km$ in altitude (see Fig.7) it is possible to estimate the air properties at each level. Thus, for each particle, a Bethe-Bloch equation is used to calculate the deposited energy due to ionization processes at the given particle energy. Finally, the fluorescence photons yield are calculated through parameterizations formulas chosen among [10] and [11]. A detailed study on the possible combinations of these formulas and their influence on the production of photons at shower axis is described elsewhere in this conference [20].

The geometry of the simulation is illustrated in Fig.8, where the telescope is positioned at the origin of the cartesian axes. The fluorescence photons travel along the line of distance R, being Rp the smaller one. The projection of primary interaction point on the surface, defines the distance D, which was sorted uniformly up to $10\,km$. $\vec{M}$ is the mirror main optical axis. We define then two angles: α is the photon elevation and σ the photon incidence angle on the mirror with respect to mirror axis.

Knowing the distances that each photon should travel we apply the attenuation factors: T^m and T^a, respectively, molecular and aerosols transmission coefficients, which can be calculated as exponential decreases like:

$$T(z,\alpha,\lambda) = e^{-\int_0^z \frac{\rho(z)dz}{sin\alpha\cdot\Lambda(\lambda)}} \qquad (2)$$

where z is the height above the detector, α is the photon elevation angle, $\rho(z)$ the density at altitude z and $\Lambda(\lambda)$ is the extinction length, which is a function of wavelength

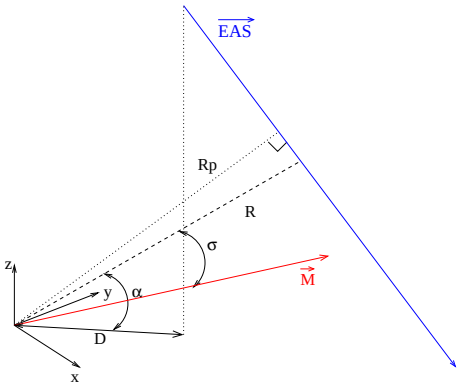

Fig. 8. Shower geometry and mirror orientation. The telescope is placed at the origin and the mirror main optical axis is aligned with $\vec{M}$

for molecular scatters and nearly a constant for aerosols [21], [22]:

$$\Lambda^m(\lambda) = (2974\ g/cm^2)\cdot(\frac{\lambda}{400\,nm})^4 \qquad (3)$$

$$\Lambda^a(\lambda = 360\,nm) \sim 20\,km \qquad (4)$$

As the photons are emitted isotropically, their fraction directed towards the telescope is given by the ratio between the mirror solid angle to the total ($\Omega_{mirr}/4\pi$). Therefore, multiplying the number of photons at the shower axis by the transmition coefficients and the solid angle fraction, we can find the number of photons impinging the telescope:

$$N_\gamma^{tel} = Y\cdot\Delta x\cdot T^m\cdot T^a\cdot\frac{\Omega_{mirr}}{4\pi} \qquad (5)$$

In the following graphics, we show the results for some selected energies. The histograms show distributions of important quantities to design the experiment, respectively, from the left to the right:

1) Distribution of shower maximum elevations for events with at least one photon impinging at the mirror. The mean of these distributions indicate the ideal alignment for MonRAt at a given energy. Notice the experiment trigger energy at $E = 10^{17} eV$;
2) Distribution of least photon distance (Rp). The lowest global Rp gives the smallest transit time of photons through the PMT: for instance, an EAS with $Rp = 1\ km$ will shine the photocathode in $233\ ns$ and suposing a vertical incidence, which is the most critical situation, it gives the time difference of $29.1\ ns$ between neighboring pixels. The MPDs were designed to have time resolution of $5\ ns$;
3) Distribution of number of photons arriving at the telescope, only for showers with at least one photon impinging the mirror. These histograms were important to design the pre-amplifiers and to set dynamic range of MPDs in terms of photon multiplicity at the mirror.

These results were important for designing the acquisition system and the dynamic range of the experiment.

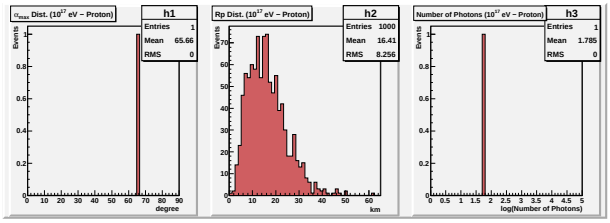

Fig. 9. Distributions for 10^3 proton showers of $10^{17}\,eV$.

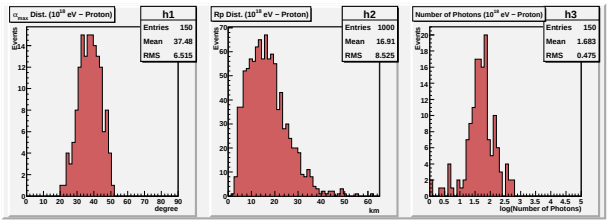

Fig. 10. Distributions for 10^3 proton showers of $10^{18}\,eV$.

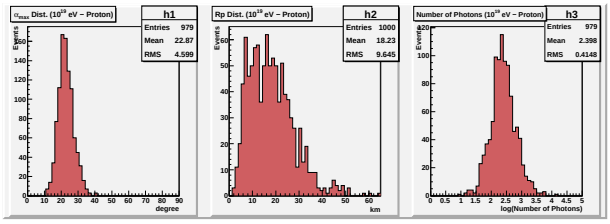

Fig. 11. Distributions for 10^3 proton showers of $10^{19}\,eV$.

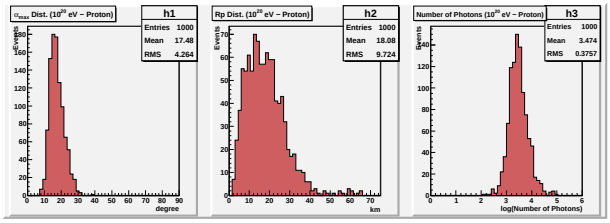

Fig. 12. Distributions for 10^3 proton showers of $10^{20}\,eV$.

Using a spherical mirror with $13.8\,cm$ of diameter and $39.2\,cm$ of curvature radius, we obtain 3° for the PMT angle of view and the solid angle viewed by one pixel is $\Omega_{pix} = 1.4 \times 10^{-4}\,srad$. One pixel views a shower with maximum depth $1\,km$ away developing for $22.2\,ns$ in $6.65\,m$. A vertical proton shower of $10^{18}\,eV$ produces 10^8 electrons in the maximum depth. The S/N ratio is proportional to the mirror diameter and inversely proportional to $\sqrt{\Omega_{pix}}$, so we estimate a very high S/N ratio per pixel of about 10^6 for such energy.

IV. Conclusions

We presented the design of the MonRAt detector and its expected performance for the detection of fluorescence radiation generated by EAS particles of primary energies greater than $10^{17}\,eV$. Studies about the detector optical properties, details for the electronics and the simulations performed to better understand the MonRAt telescope has been presented. This detector will be soon able to measure real events, detecting for the first time fluorescence radiation in Brazilian night skies.

V. Aknowledgements

The financial support for this work was given by the Brazilian foudations CNPq (Conselho Nacional de Desenvolvimento Científico e Tecnológico) and FAPESP (Fundação de Amparo à Pesquisa do Estado de São Paulo). The authors are thankful to our colleagues at UFABC, CBPF and UNICAMP for the laboratorial facilities used in the development of this work.

References

[1] T. Hara *et al.*, *Acta Phys. Acad. Sci. Hung.*, **29**, Suppl. 3 (1970) 361.
[2] R. M. Baltrusaitus *et al.*, *Nucl. Instr. and Meth. in Phys. Res.:* **A240** (1985) 410.
[3] T. Abu-Zayyad *et al.*, *Nucl. Instr. and Meth. in Phys. Res.:* **A450** (2000) 253.
[4] J. Abraham *et al.*, *Nucl. Instr. and Meth. in Phys. Res.:* **A523** (2004) 50;
[5] M. Fukushima, *Prog. Theo. Phys. Suppl.*, **151** (2003) 206.
[6] L. Scarsi, *Proc. 27th Int. Cosmic Ray Conf.*, Hamburg (2001) 839.
[7] F. W. Stecker *et al.*, *Nucl. Phys.* **B139** (2004) 433.
[8] A. N. Bunner, *Cosmic Ray Detection by Atmospheric Fluorescence*, PhD Thesis, Cornell Univ. (Feb. 1967).
[9] G. Davidson and R. O'Neil, *J. Chem. Phys.*, **41** (1964) 3946.
[10] K. Kakimoto, *et al.*, *Nucl. Instr. and Meth. in Phys. Res.:* **A372** (1996) 527.
[11] M. Nagano *et al.*, *Astropart. Phys.*, **20** (2003) 293; **22** (2004) 235.
[12] J. W. Beltz *et al.*, *Astropart. Phys.*, **25** (2006) 129.
[13] P. Collin *et al.*, astroph/06121110.
[14] V. de Souza, G. Medina-Tanco and J. A. Ortiz, *Astropart. Phys.*, **25** (2006) 129.
[15] M. A. Leigui de Oliveira *et al.*, *Monitor de Radiação Atmosférica*, XXIX ENFPC, SBF, São Lourenço (2008), Brazil.
[16] Hamamatsu Photonics K.K., http://www.hamamatsu.com
[17] D. Heck, J. Knapp, J. N. Capdevielle, G. Schatz, and T. Thouw, Report **FZKA 6019** (1998), Forschungzentrum Karlsruhe; http://www-ik.fzk.de/ heck/publications/fzka6019.pdf
[18] R. S. Fletcher *et al.*, *Phys. Rev. D*,**D50** (1994) 5710.
[19] Intergovernmental Panel on Climate Change, *IPCC Report*, (2001), http://www.ipcc.ch
[20] M.A. Leigui de Oliveira, C.J. Todero Peixoto, M.S.A.B. Leão, *The ionization energy deposit in the atmosphere and the fluorescence light generation at shower axis*, 31st ICRC, Lodz, Session: HE.1.4 (2009). ID=98.
[21] E. C. Flowers, R. A. McCormick and J. Kurfis,*J. Appl. Meteorology*, **8** (1969) 955.
[22] P. Sokolsky, *Proc. of Int. Sym. on EHECRs: Astrophysics and Future Observatories*, Ed. M. Nagano (1996) 253.